

Adiabatic Waves of Gasless Combustion: 3D Simulation

T.P. Ivleva, and A.G. Merzhanov
Institute of Structural Macrokinetics and Materials Science,
Russian Academy of Sciences,
Chernogolovka, Moscow, 142432 Russia
tanja@ism.ac.ru

In the present study, discussion of the structure and mechanism of the spinning combustion regimes in the gasless systems is based on the results of calculations performed by the authors. Generally, spinning combustion waves manifest themselves as one or several bright hot spots that move alongside a screw trajectory over the sample surface [1-3]. (Hot spot is a zone where the reaction rate is maximal and where temperature is much greater than temperature under the adiabatic conditions). The results reported herein belong to the established regimes. The question on the number of the periods obtained during calculation that could ensure establishment of the stationary regime has not been yet answered. In our opinion, the regime can be considered settled after its behaviour has been retained for 15-20 periods.

Let's consider a thermally insulated cylindrical sample prepared from a mixture of two powdered reactants. The initial components and the reaction products are assumed to be thermally homogeneous solids. Let's assume that an exothermic reaction of these reagents yields only solid products (on retention of sample weight). Such an exothermic process (when the involvement of gases can be neglected) is termed gasless combustion. We will make use of the following system of three-dimensional (3D) equations:

$$c\mathbf{r}_0 \frac{\partial T}{\partial t} = \mathbf{l} \left(\frac{\partial^2 T}{\partial r^2} + \frac{1}{r} \frac{\partial T}{\partial r} + \frac{1}{r^2} \frac{\partial^2 T}{\partial \mathbf{j}^2} + \frac{\partial^2 T}{\partial h^2} \right) + \mathbf{r}_0 Q \frac{\partial \mathbf{h}}{\partial t},$$

$$\frac{\partial \mathbf{h}}{\partial t} = \begin{cases} k_0 (1-\mathbf{h}) \exp\left(-\frac{E}{RT}\right) & \text{for } \mathbf{h} < 1, \\ 0 & \text{for } \mathbf{h} \geq 1, \end{cases}$$

with the following boundary conditions:

$$t = 0: T = T_0, \mathbf{h} = 0,$$

$$t > 0, r = r_0: \mathbf{l} \frac{\partial T}{\partial r} = 0,$$

$$h = 0: \mathbf{l} \frac{\partial T}{\partial h} = 0,$$

$$h = h_0: \begin{cases} T = T_b & \text{for } t \leq t_{\text{ign}}, \\ \mathbf{l} \frac{\partial T}{\partial h} = 0 & \text{for } t > t_{\text{ign}}. \end{cases}$$

Here T is temperature, T_0 is the initial sample temperature, $T_b = T_0 + Q/c$ is the temperature of burning; η is the conversion depth for a deficient component, ρ_0 is the mean density; t is time, t_{ign} is the time of ignition; r, φ, h are the cylindrical coordinates; r_0, h_0 are the radius and height of cylinder; c is the heat capacity; λ is the thermal conductivity; k_0 is the pre-exponential factor; Q is the reaction heat; E is the activation energy for a given reaction; and R is the universal gas constant. Ignition is initiated at the top of the sample, so that front of combustion propagates downward. The problem was solved by finite difference method in the dimensionless form. The dimensionless parameters were

$$\mathbf{q} = \frac{(T - T_*)E}{RT_*^2}, \quad t_* = \frac{cRT_*^2}{k_0EQ} \exp\left(\frac{E}{RT_*}\right), \quad \mathbf{t} = \frac{t}{t_*}, \quad h_*^2 = \frac{I t_*}{c r_0}, \quad x = \frac{r}{h_*}, \quad z = \frac{h}{h_*}.$$

The non-uniform spatial grid with the non-fixed number of nodes was adapted to the solution by the nod concentration in the region of the front and by 'the sample growing' from the reagent side and 'cutting-off' of the remote from the front portion of the products. Our calculation procedure for 3D modeling allowed us to solve the above system of equations by using only a PC. The obtained data provide an insight into the 'inner' structure of spinning wave.

The spinning waves arise owing to the fact that the planar reaction front becomes unstable with respect to spatial perturbations. The range of system parameters within which the reaction front loses its stability is given by the following approximate expression (obtained upon numerical solution of the 1D problem [4]):

$$\alpha_{\text{st}} = 9.1 \frac{cRT_b^2}{EQ} - 2.5 \frac{RT_b}{E} < 1.$$

where α_{st} is some combination of reaction parameters. For a given pair of reagents, the higher is α_{st} , the higher is T_b .

In our calculations, we used α_{st} and the dimensionless radius $R_0 = r_0 \left[\frac{k_0 r_0 EQ}{I RT_b^2} \exp\left(-\frac{E}{RT_b}\right) \right]^{1/2}$ as governing parameters. The dimensionless radius R_0 gives the number of reaction zones that could be stowed within the sample radius r_0 .

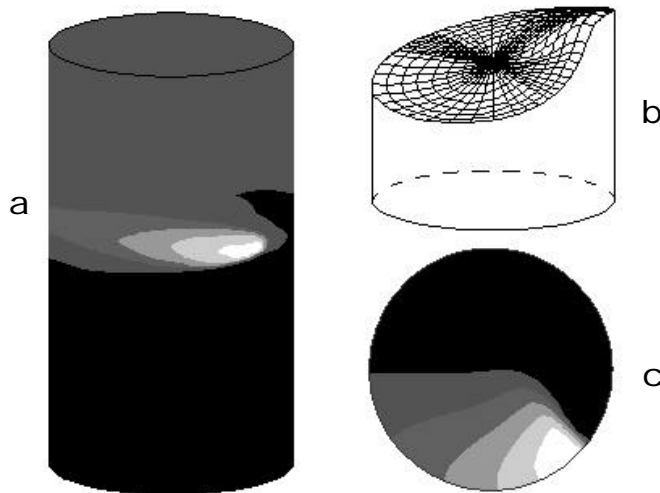


Figure 1 Single-spot mode of steady spinning wave: (a) temperature distribution over the sample surface, (b) reaction front structure (a multitude of the points, in which the limiting component is half-converted, is taken for the combustion front), and (c) temperature distribution over a normal cross section at a point with maximum T . Brighter areas correspond to higher T ; in black areas, $T < T_b$.

The so-called single-spot spinning wave is most widespread. In the simplest case (Fig. 1), the process develops steadily: the front profile remains permanently curved and just propagate downward alongside a screw trajectory at a constant velocity. Spinning waves with two spots on the surface are also possible. According to our calculations, these waves emerge in cylindrical samples with a relatively small R_0 . With increasing R_0 , the spinning waves loose their stability: although remaining periodic, they undergo numerous transformations during one period. The motion of hot spots in different modes is illustrated in Fig. 2.

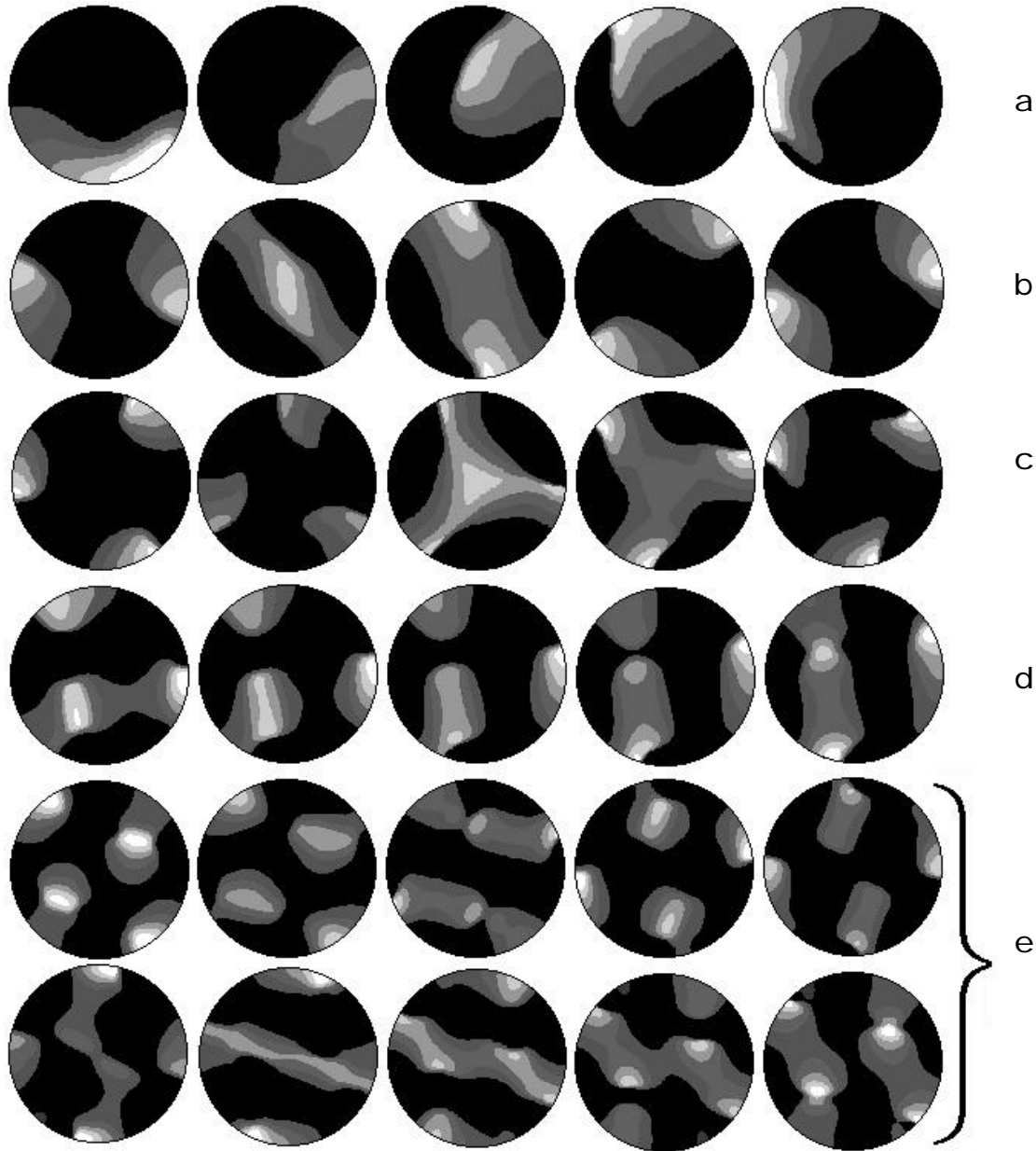


Figure 2 Image sequences illustrating one period of the motion of hot spots at different R_0 for $\alpha_{st} \approx 0.9$: (a) unsteady single-spot wave ($R_0 = 60$), (b) unsteady symmetric two-spot wave ($R_0 = 40$), (c) unsteady symmetric three-spot wave ($R_0 = 80$), (d) asymmetric flickering wave ($R_0 = 60$), and (e) unsteady multi-spot wave ($R_0 = 80$). Temperature distribution is shown for a normal cross section at a point with a maximum value of T . Sample

cross sections are normalized to equal size (irrespective of real value of radius R_0). Brighter areas correspond to higher T ; in black areas, $T < T_b$.

With an increase in R_0 , the wave propagation becomes periodic but unsteady. Our data show that, for an unsteady single-spot spinning wave (Fig. 2a), the spot size, velocity of motion alongside the screw trajectory, and temperature also undergo pulsation. When the hot spot is extended, it reaches the central area (i.e., temperature at the center increases) and then shrinks again (temperature at the sample center goes down) (Fig. 2a). As a result, T and instantaneous wave velocity at the sample axis oscillate around some mean value. Such a pulsation was observed experimentally [5]. When the hot spot shrinks (toward the surface), a heat flux from the spot is insufficient for initiating the reaction at the sample axis (because R_0 is relatively large). But instead, a zone of heat-affected mixture is formed. As the hot spot approaches this zone, it initiates the reaction front in this zone. Depending on α_{st} and R_0 , a maximum value of T may be attained at any point of the front, including the sample center. When reaction is completed in the center, the hot spot shrinks toward the sample surface, to the areas with still unreacted mixture. In this way, the spot structure and velocity of its motion undergo periodic changes (not multiple of 2π).

A simplest symmetric spinning wave comprises two diametrically opposite hot spots. Their motion may be accompanied either (i) by steady propagation along the sample axis (for small R_0 and insignificant deviation from the stability limit) or (ii) by burning down the central area in a pulsation mode. In the latter case, the motion of hot spots becomes unsteady (Fig. 2b). Propagation of hot spots over the surface gradually decelerates until fast burning (flare) of preheated mixture in the central area. This is followed by the transfer of released heat to the near-surface areas, which increases the reaction rate at the surface. With increasing separation from the hot central zone, the temperature of hot spots and their velocity decrease again. The process is repeated periodically.

We observed similar spinning waves with three hot spots. In this case (Fig. 2c), the temperature of spots simultaneously decreases, while the central area is heated (by heat transfer) until a flare that rises the temperature of the surface spots. With increasing T , the spots begin to move faster, and *vice versa*.

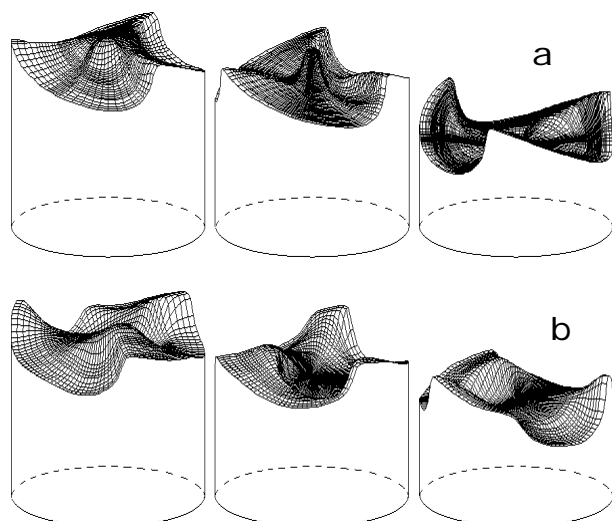


Figure 3 Image sequences showing the evolution of reaction front: (a) unsteady symmetric three-spot wave and (b) unsteady asymmetric three-spot wave.

The evolution of front structure during one period is illustrated in Fig. 3a. It follows that the reaction front in the center gradually retards while the area of retardation becomes narrower. After the last third of period, the front structure becomes identical to the initial one (although it is shifted along z and φ).

There also exist another three-spot mode—the asymmetric one. In this case, three spots alternatively leave the surface toward the sample center. The spot that is inside coalesces with one of two near-surface spots, thus giving rise to two new spots. One of these two spots appears at the surface, while another moves toward the third one (Fig. 2d). As a result, we observe three spots that alternatively flare and fade on the surface. The evolution of reaction front is illustrated in Fig. 3b.

In case of the multispot wave—a most complicated of observed propagation modes—the spots are periodically taken off (in pairs) from the surface and move toward the sample center. In this case, they interact each with other as well as with the spots that remain in the near-surface layer, which is accompanied by bright flaring or fading. The spots bifurcate and then coalesce (Fig. 2e).

The mean velocity of the 3D front propagation through the cylinder was determined by the following formula:

$$\bar{u} = \frac{l}{p R_0^2 (t_k - t_0)} \left(\iiint_V h(x, \mathbf{j}, z, t_k) dV - \iiint_V h(x, \mathbf{j}, z, t_0) dV \right),$$

where t_k, t_0 is the time for the beginning and completing the process in this stage respectively, V is the cylinder volume. As mentioned above, the value for the velocity of combustion front moving along the cylinder axis can pulsate or remain constant. Let us consider behavior of the mean (along the cylinder diameter) temperature expressing by the following formula

$$\bar{q}(z, t) = \frac{l}{p R_0^2} \int_0^{R_0} \int_0^{2p} q(x, \mathbf{j}, z, t) d\mathbf{j} dr. \text{ The distribution of } \bar{q}(z, t) \text{ along the sample is similar to}$$

the distribution of the temperature at 1D stationary front propagation. In this case, the amplitude of the mean temperature oscillation is very low even at very high amplitude of temperature oscillations in the reaction zone on the cylinder axis and generatrix. This is associated with temperature redistribution along the sample diameter forming the hot spots during 3D spinning combustion. The normal front velocity would be supposed to form in a way like that in the stationary adiabatic situation. However for the specific spinning combustion, a slight decrease in the mean velocity of propagation (up to 10—15%) with increasing the cylinder radius may take place.

Also the non-uniqueness of combustion modes was found. The areas of existence for these modes have been determined.

1. A.G. Merzhanov, A.K. Filonenko and I.P. Borovinskaja, Dokl. Akad. Nauk SSSR, **208**, 892 (1973).
2. Yu.M. Maksimov et al., Fiz. Goreniya Vzryva, **3**, 156 (1979).
3. J. Puszynski et al., Z. Naturforsch, **43a**, 1017 (1988).
4. K. G. Shkadinsky, B.I. Khaikin and A.G. Merzhanov, Fiz. Goreniya Vzryva, **1**, 15 (1971).
5. A.V. Dvoryankin and A.G. Strunina, Fiz. Goreniya Vzryva, **2**, 41 (1991).